

Supplementary Materials and Methods

Genomic analysis reveals shared genes and pathways in human and canine angiosarcoma

Sample collection

Samples were collected from dogs referred for treatment at the University of Minnesota (UMN) Veterinary Medical Center, from samples submitted to the Modiano laboratory for diagnostic assessment and/or use in research (n = 34), from cases seen at the North Carolina State University (NCSU) Veterinary Hospital (n = 8), or from diagnostic samples sent to Antech Diagnostics (n = 5). Cases where date of diagnosis was known (n = 36), were diagnosed between 2000 and 2014. Tumor samples were either frozen (n = 17), or formalin-fixed and paraffin-embedded (FFPE, n = 30, **Table S1**). Procedures involving animal use were approved by the Institutional Animal Care and Use Committees at the Broad Institute, UMN, or NCSU.

DNA extraction

FFPE tumor samples were macrodissected by microtome to select for regions of high tumor cell density, and tumor DNA was prepared using the Qiagen QIAamp DNA FFPE Tissue Kit. DNA from frozen tumor tissue and germline DNA from whole blood were prepared using the Qiagen DNeasy Blood and Tissue Kit. The DNA was then eluted into nuclease-free purified water. DNA concentration was determined using the NanoDrop microvolume spectrophotometer (ThermoFisher Scientific) and/or the Quant-iT PicoGreen system (Invitrogen).

Library construction

1 μ g of DNA from each tumor and normal sample was diluted in Tris-EDTA (TE) buffer for sonic fragmentation. Samples were fragmented to a target size of 500bp using a Covaris ultrasonicator (Covaris). Fragments were cleaned and subject to size selection using Agencourt AMPure XP magnetic beads (Beckman Coulter). Select samples were visualized using the Agilent BioAnalyzer to check the distribution of fragment sizes. The Kapa Hyper Prep Kit was used for library construction (Kapa Biosystems). Briefly, size-selected DNA fragments were subject to end-repair and A-tailing reactions, followed by attachment of adaptors in preparation for molecular barcoding. Fragments were purified using Agencourt AMPure XP magnetic beads between reactions. NEBNext Multiplex Oligos for Illumina (New England BioLabs) were then used to barcode the individual libraries following product guidelines.

Amplification of samples

The 66 overamplified samples had significantly fewer mutations than the 28 samples amplified using the recommended number of PCR cycles (mean mutational burden per tumor/normal pair = 21.4 vs 31.3, p = 0.02) and significantly lower estimated library size (number of unique molecules; p < 0.001; **Table S2**) consistent with a lower library complexity in the overamplified samples. Thus, in the overamplified samples, we are likely underpowered to discover variants, leading to a more conservative set of mutations. We note that all significantly mutated genes discovered during data analysis are mutated in both standard and overamplified samples, with the sole exception of *ATP5PD*, which was only found in the overamplified samples (**Figure S2**).

Exome capture

Custom blocking oligonucleotides were designed complementary to the barcode sequences and synthesized by Integrated DNA Technologies (IDT). Briefly, the amplified libraries were incubated with the SeqCap EZ probes, blocking oligos, and Roche Developer Reagent (in place of human Cot-1 DNA), for 60 hours in a thermocycler (Eppendorf). Captured DNA was then recovered and washed using SeqCap-EZ Capture Beads. The captured library was amplified via ligation-mediated (LM)-PCR for the recommended 14 cycles, and the amplified captured library washed using AMPure XP magnetic beads. qPCR using primers for specific targeted regions and a negative control region that was not targeted was performed to test enrichment of a subset of the captured libraries for using the LightCycler 480 instrument (Roche).

Somatic variant calling

We called variants in the GATK3 MuTect2 and GATK4 Mutect2 versions, with the addition of the `--dontUseSoftClippedBases` option. Prior to using this setting, we saw a large number of artifactual indels being called in our FFPE samples. These indels were being called with the only support for the variant being the ends of soft-clipped reads. A similar artifact has been reported in WGA TCGA data (1). We found no significant difference in the total number of mutations ($p_{t\text{-test}} = 0.76$) or percent of indels ($p = 0.95$) between frozen ($n = 17$) and FFPE ($n = 30$) samples in the final somatic mutation call set.

Variants for the panel of normals were called as recommended in the GATK3 workflow, using `--artifactDetectionMode` in MuTect2, and the calls from the normal samples were merged using CombineVariants, keeping any variant that was called in two or more dogs. All preprocessing was performed using GATK version 3.6.0 (2). BQSR was performed using a set of 19,112,082 known canine SNP positions drawn from multiple sources, including SNPs discovered by the Lindblad-Toh (3,4) and Axelsson labs (5), those included on the Affymetrix Axiom Canine HD array, and those contained in the DoGSD database (6).

Using GATK4, we again used the default Mutect2 parameters, with the addition of the `--dontUseSoftClippedBases` option. We then applied the FilterMutectCalls tool to this set of variant calls, using default cutoffs, with the exception of increasing the stringency of the median read position filter to ten, and specifying a unique alternate allele read count of four. The FilterByOrientationBias tool (labeled “experimental”) was also applied, using the “G,T” setting (for oxidation artifacts) for all samples, and the “C,T” setting for FFPE-preserved samples.

Somatic copy number aberration calling

Somatic copy number alterations in tumors compared to the matched normal were called in the exome data using VarScan2 (7) followed by circular binary segmentation to translate intensity measurements into regions. Recurrent SCNAs were then identified using Gistic2 (8) using default options and a cutoff threshold of 10000 for “max seg”.

RNA-sequencing

Total RNA was isolated from tissue samples using the TriPure Isolation Reagent (Roche Applied Science), and the RNeasy Mini Kit (Qiagen) was used for clean-up according to the manufacturer's instructions. Briefly, the TruSeq RNA sample preparation kit (Illumina) and a HiSeq 2000 or 2500

sequencing system (Illumina) were used to generate Illumina sequencing libraries. Each sample was sequenced to a targeted depth of approximately 20 – 80 million paired-end reads with mate-pair distance of 50 bp. Primary analysis and demultiplexing were performed using CASAVA software version 1.8.2 (Illumina) to verify the quality of the sequence data. The end result of the CASAVA workflow was demultiplexed into FASTQ files for analysis. Bioanalyzer quality control and RNA-seq were performed at the University of Minnesota Genomics Center (UMGC) or at the Broad Institute.

Comparative pathway analysis

For the comparative pathway analysis, gene names and Ensembl IDs were mapped to known gene IDs within the DAVID tool. The 1092 total canine mutations mapped to 951 human gene IDs in the DAVID tool. The 1958 total mutated human genes mapped to 1934 gene IDs. The union of all mutated genes in both cohorts (n=2929) mapped to 2617 IDs.

Construction of lollipop plots

Canine variants were lifted over to the human genome (hg19) using the UCSC LiftOver tool (9). Plots were created using the MutationMapper function at CBioPortal. Six canine TP53 variants were not plotted due to mismatch of the reference allele in the canine and human genomes.

Supplementary discussion

Significantly mutated genes in the canine cohort

The significantly mutated genes in our canine cohort which were less frequently mutated still may give us important insight into disease pathophysiology. *RASA1* is a negative regulator of the RAS and MAPK pathways, and plays an important role in vascular formation(10,11). Germline *RASA1* mutations can cause capillary malformation - arteriovenous malformation syndrome(12). Somatic mutations in this gene have been found in a subset of human basal cell carcinomas, and expression has been correlated with survival in invasive ductal breast carcinomas and hepatocellular carcinomas(13,14). Three out of four of the mutations in this gene in our dataset are nonsense mutations. In the Angiosarcoma Project data, one case has a missense mutation and one case a nonsense mutation in *RASA1*. *ORC1* is part of the DNA replication complex(15). *ARPC1A* plays an important role in regulating the actin cytoskeleton, which functions in the migration and invasiveness of pancreatic carcinoma cells(16). *ATP5H* is a mitochondrial ATP synthase(15). One study found that ATP5H interacts with PLCB1, which promotes cellular proliferation(17), while another study found that loss of ATP5H activity led to a stem cell-like phenotype, invasiveness, and resistance to therapy(18). It is notable that this gene was also significantly mutated in golden retriever B-cell lymphomas in one of our earlier exome sequencing studies(19).

Mutational burden by tumor location

In the human data, mutation rates are significantly different between different tumor locations, with head and neck angiosarcomas having a much higher mutational burden, as reported by Painter, et al (20). It is possible that the higher mutational burden in these tumors is due to UV exposure. It would be interesting to compare these findings to canine cutaneous and subcutaneous angiosarcomas, which were not included in this study. In the canine data, no significant difference was found between mutational burden by tumor location, however, all included cases were visceral tumors. It makes sense

that the golden retrievers have a lower overall somatic mutation burden than humans, as they likely have a much higher germline risk burden, given the high incidence of angiosarcoma in the breed.

RNA-seq survey of angiosarcoma in multiple breeds

We took advantage of the broader cohort of canine angiosarcoma cases in the RNA-seq data to look at the distribution of SMGs across multiple breeds, and found that frequent *TP53* and *PIK3CA* mutations are not unique to the golden retriever genetic background, but are also found in other breeds, as reported by Wang, *et al* (21).

Comparative pathway analysis

The most highly enriched category in both the dog and human data was glycoproteins, likely because this broad category actually encompasses many of the protein families that are noted as enriched on their own. Glycoproteins are a large category of proteins which have been post-translationally modified to carry a carbohydrate group (22), and play a role in numerous cellular processes, including playing an important role in the extracellular signalling, through membrane receptors and secreted proteins.

While *PLCG1* has been reported as frequently mutated in human angiosarcomas, particularly in secondary tumors (23), none of the cases with *PLCG1* mutations in the current Angiosarcoma Project had previous radiation therapy (two had radiation as part of their current treatment for angiosarcoma), perhaps suggesting that mutations in this gene are not as rare in primary angiosarcomas as previously thought.

References

1. MuTect2 Insertion Artifacts [Internet]. National Cancer Institute Genomic Data Commons. 2016 [cited 2018 Sep 28]. Available from: <https://gdc.cancer.gov/content/mutect2-insertion-artifacts>

2. Van der Auwera GA, Carneiro MO, Hartl C, Poplin R, Del Angel G, Levy-Moonshine A, et al. From FastQ data to high confidence variant calls: the Genome Analysis Toolkit best practices pipeline. *Curr Protoc Bioinformatics*. 2013;43:11.10.1–33.
3. Lindblad-Toh K, Wade CM, Mikkelsen TS, Karlsson EK, Jaffe DB, Kamal M, et al. Genome sequence, comparative analysis and haplotype structure of the domestic dog. *Nature*. 2005;438:803–19.
4. Vaysse A, Ratnakumar A, Derrien T, Axelsson E, Rosengren Pielberg G, Sigurdsson S, et al. Identification of genomic regions associated with phenotypic variation between dog breeds using selection mapping. *PLoS Genet*. 2011;7:e1002316.
5. Axelsson E, Ratnakumar A, Arendt M-L, Maqbool K, Webster MT, Perloski M, et al. The genomic signature of dog domestication reveals adaptation to a starch-rich diet. *Nature*. 2013;495:360–4.
6. Bai B, Zhao W-M, Tang B-X, Wang Y-Q, Wang L, Zhang Z, et al. DoGSD: the dog and wolf genome SNP database. *Nucleic Acids Res*. 2015;43:D777–83.
7. Koboldt DC, Zhang Q, Larson DE, Shen D, McLellan MD, Lin L, et al. VarScan 2: somatic mutation and copy number alteration discovery in cancer by exome sequencing. *Genome Res*. 2012;22:568–76.
8. Mermel CH, Schumacher SE, Hill B, Meyerson ML, Beroukhir R, Getz G. GISTIC2.0 facilitates sensitive and confident localization of the targets of focal somatic copy-number alteration in human cancers. *Genome Biol*. 2011;12:R41.
9. Kent WJ, Sugnet CW, Furey TS, Roskin KM, Pringle TH, Zahler AM, et al. The human genome browser at UCSC. *Genome Res*. 2002;12:996–1006.
10. Pamonsinlapatham P, Hadj-Slimane R, Lepelletier Y, Allain B, Toccafondi M, Garbay C, et al. p120-Ras GTPase activating protein (RasGAP): a multi-interacting protein in downstream signaling. *Biochimie*. 2009;91:320–8.
11. Henkemeyer M, Rossi DJ, Holmyard DP, Puri MC, Mbamalu G, Harpal K, et al. Vascular system defects and neuronal apoptosis in mice lacking ras GTPase-activating protein. *Nature*. 1995;377:695–701.
12. Eerola I, Boon LM, Mulliken JB, Burrows PE, Domp Martin A, Watanabe S, et al. Capillary malformation-arteriovenous malformation, a new clinical and genetic disorder caused by RASA1 mutations. *Am J Hum Genet*. 2003;73:1240–9.
13. Liu Y, Liu T, Sun Q, Niu M, Jiang Y, Pang D. Downregulation of Ras GTPase-activating protein 1 is associated with poor survival of breast invasive ductal carcinoma patients. *Oncol Rep*. 2015;33:119–24.
14. Chen Y-L, Huang W-C, Yao H-L, Chen P-M, Lin P-Y, Feng F-Y, et al. Down-regulation of RASA1 Is Associated with Poor Prognosis in Human Hepatocellular Carcinoma. *Anticancer Res*. 2017;37:781–5.

15. O'Leary NA, Wright MW, Brister JR, Ciuffo S, Haddad D, McVeigh R, et al. Reference sequence (RefSeq) database at NCBI: current status, taxonomic expansion, and functional annotation. *Nucleic Acids Res.* 2016;44:D733–45.
16. Laurila E, Savinainen K, Kuuselo R, Karhu R, Kallioniemi A. Characterization of the 7q21-q22 amplicon identifies ARPC1A, a subunit of the Arp2/3 complex, as a regulator of cell migration and invasion in pancreatic cancer. *Genes Chromosomes Cancer.* 2009;48:330–9.
17. Piazzini M, Blalock WL, Bavelloni A, Faenza I, D'Angelo A, Maraldi NM, et al. Phosphoinositide-specific phospholipase C β 1b (PI-PLC β 1b) interactome: affinity purification-mass spectrometry analysis of PI-PLC β 1b with nuclear protein. *Mol Cell Proteomics.* 2013;12:2220–35.
18. Song K-H, Kim J-H, Lee Y-H, Bae HC, Lee H-J, Woo SR, et al. Mitochondrial reprogramming via ATP5H loss promotes multimodal cancer therapy resistance. *J Clin Invest.* 2018;128:4098–114.
19. Elvers I, Turner-Maier J, Swofford R, Koltoonian M, Johnson J, Stewart C, et al. Exome sequencing of lymphomas from three dog breeds reveals somatic mutation patterns reflecting genetic background. *Genome Res.* 2015;25:1634–45.
20. Painter C, Jain E, Dunphy M, Anastasio E, McGillicuddy M, Stoddard R, Thomas B, Balch Sara, Anderka K, Larkin K, Lennon N, Chen Y-L, Zimmer A, Baker EO, Maiwald S, Lapan J, Hornick JL, Raut C, Demetri G, Lander ES, Golub T. High mutation burden and response to immune checkpoint inhibitors in angiosarcomas of the scalp and face. 2018.
21. Wang G, Wu M, Maloneyhuss MA, Wojcik J, Durham AC, Mason NJ, et al. Actionable mutations in canine hemangiosarcoma. *PLoS One.* 2017;12:e0188667.
22. Wilkinson A, McNaught A. IUPAC Compendium of Chemical Terminology, (the“ Gold Book”). International Union of Pure and Applied Chemistry. 1997;
23. Murali R, Chandramohan R, Möller I, Scholz SL, Berger M, Huberman K, et al. Targeted massively parallel sequencing of angiosarcomas reveals frequent activation of the mitogen activated protein kinase pathway. *Oncotarget.* 2015;6:36041–52.

Supplementary Tables and Figures

Genomic analysis reveals shared genes and pathways in human and canine angiosarcoma

Table S1 - Cohort metadata

Case ID	Tissue preservation	Location	Nonsynonymous mutations	Sex	Age
1	fixed	liver	15	F	10
2	frozen	spleen	22	M	9
3	fixed	heart	35	F	11
4	frozen	spleen	26	F	10
5	fixed	liver	30	M	11
6	frozen	spleen	22	M	10
7	fixed	liver	17	M	6
8	fixed	heart	31	F	5
9	frozen	spleen	17	F	11
10	fixed	heart	10	F	12
11	frozen	spleen	26	M	7
12	fixed	heart	22	M	10
13	fixed	spleen	13	F	8
14	fixed	spleen	11	F	11
15	fixed	heart	24	F	15
16	frozen	spleen	37	M	10
17	frozen	heart	33	F	8
18	frozen	spleen	13	M	9
19	frozen	spleen	17	M	3
20	frozen	heart	21	M	9
21	fixed	heart	64	F	8
22	fixed	heart	35	M	12
23	frozen	spleen	5	F	11
24	fixed	liver	37	F	10
25	fixed	liver	27	M	12
26	frozen	spleen	3	F	14
27	frozen	spleen	41	F	9
28	frozen	heart	45	M	9
29	frozen	spleen	26	M	13
30	fixed	spleen	3	M	NA
31	fixed	spleen	43	M	NA
32	fixed	spleen	22	F	NA

33	fixed	spleen	7	M	NA
34	fixed	spleen	13	M	NA
35	fixed	heart	46	F	11
36	fixed	heart	16	F	9
37	fixed	heart	149	F	15
38	fixed	spleen	13	M	NA
39	fixed	heart	33	F	NA
40	fixed	heart	16	F	NA
41	frozen	heart	30	M	NA
42	fixed	liver	23	M	NA
43	fixed	spleen	46	F	NA
44	frozen	spleen	14	F	4
45	fixed	liver	22	F	5
46	fixed	liver	41	F	13
47	fixed	unknown, likely heart	1	F	11

Table S2 - Library preparation, amplification, and complexity

Case ID	Tumor/Normal	Sequencing depth	Input DNA	Overamplified	Tissue preservation	Nonsynonymous mutations	Library size
1	Normal	49	1000	Yes	EDTA		134561459
1	Tumor	53	1000	Yes	fixed	15	38155922
2	Normal	71	1000	Yes	EDTA		226048914
2	Tumor	91	1000	Yes	frozen	22	136254048
3	Normal	73	1000	Yes	EDTA		134978503
3	Tumor	26	1000	Yes	fixed	35	20412528
4	Normal	61	1000	Yes	EDTA		231846809
4	Tumor	99	1000	Yes	frozen	26	103917348
5	Normal	51	1000	Yes	EDTA		370312244
5	Tumor	41	1000	Yes	fixed	30	32017163
6	Normal	63	1000	Yes	EDTA		225490375
6	Tumor	84	1000	Yes	frozen	22	130755435
7	Normal	53	1000	Yes	EDTA		269484482
7	Tumor	89	1000	Yes	fixed	17	73256644
8	Normal	80	1000	Yes	EDTA		268801501
8	Tumor	75	1000	Yes	fixed	31	81740488

9	Normal	62	1000	Yes	EDTA		281443846
9	Tumor	101	1000	Yes	frozen	17	210031996
10	Normal	83	1000	No	EDTA		355514908
10	Tumor	78	1000	No	fixed	10	69807014
11	Normal	68	NA	No	EDTA		277032267
11	Tumor	126	1000	No	frozen	26	324015250
12	Normal	62	1000	Yes	EDTA		221713689
12	Tumor	55	1000	Yes	fixed	22	49450048
13	Normal	43	1000	Yes	EDTA		203071580
13	Tumor	91	1000	Yes	fixed	13	144056227
14	Normal	58	1000	Yes	EDTA		177387584
14	Tumor	61	1000	Yes	fixed	11	65437960
15	Normal	75	1000	Yes	EDTA		127216800
15	Tumor	56	1000	Yes	fixed	24	40991888
16	Normal	73	1000	Yes	EDTA		141452611
16	Tumor	56	1000	Yes	frozen	37	41118918
17	Normal	62	1000	No	EDTA		223257784
17	Tumor	114	NA	No	frozen	33	147787071
18	Normal	53	1000	Yes	EDTA		171084585
18	Tumor	78	1000	Yes	frozen	13	97513922
19	Normal	69	1000	Yes	EDTA		129594138
19	Tumor	75	1000	Yes	frozen	17	91271441
19	Normal	67	1000	Yes	EDTA		110209804
20	Tumor	91	1000	Yes	frozen	21	161197314
21	Normal	64	1000	No	EDTA		293332856
21	Tumor	144	309*	No	fixed	64	161501907
22	Normal	62	1000	Yes	EDTA		123858089
22	Tumor	57	1000	Yes	fixed	35	42916453
23	Normal	54	1000	Yes	EDTA		214634405
23	Tumor	84	1000	Yes	frozen	5	163422686
24	Normal	51	1000	Yes	EDTA		130312170
24	Tumor	56	1000	Yes	fixed	37	40995053
25	Normal	62	1000	No	EDTA		232499575
25	Tumor	46	1000	Yes	fixed	27	34254483
26	Normal	74	1000	No	EDTA		159151355
26	Tumor	93	381*	No	frozen	3	128242059
27	Normal	74	1000	Yes	EDTA		100619527

27	Tumor	96	1000	Yes	frozen	41	135472727
28	Normal	90	1000	No	EDTA		229798708
28	Tumor	109	469*	No	frozen	45	196472240
29	Normal	52	1000	No	EDTA		280852929
29	Tumor	125	425*	No	frozen	26	316081507
30	Normal	69	1000	Yes	EDTA		131692351
30	Tumor	85	1000	Yes	fixed	3	100942519
31	Normal	50	1000	Yes	EDTA		118651337
31	Tumor	75	1000	Yes	fixed	43	48558498
32	Normal	59	1000	Yes	EDTA		137223693
32	Tumor	40	1000	Yes	fixed	22	25433630
33	Normal	65	1000	Yes	EDTA		116541031
33	Tumor	54	1000	Yes	fixed	7	63455690
34	Normal	60	1000	Yes	EDTA		89817007
34	Tumor	74	1000	Yes	fixed	13	44486076
35	Normal	51	1000	No	EDTA		210786142
35	Tumor	114	295*	No	fixed	46	163041517
36	Normal	27	1000	Yes	EDTA		58556571
36	Tumor	45	1000	Yes	fixed	16	56260934
37	Normal	54	1000	No	EDTA		98731048
37	Tumor	128	871*	No	fixed	149	127593218
37	Normal	67	1000	Yes	EDTA		87139774
38	Tumor	45	1000	Yes	fixed	13	31958634
39	Normal	95	NA	No	EDTA		171064700
39	Tumor	93	355*	No	fixed	33	88831176
40	Normal	54	1000	Yes	EDTA		65023743
40	Tumor	18	1000	Yes	fixed	16	16470714
41	Normal	59	1000	No	EDTA		173375722
41	Tumor	97	480*	No	frozen	30	119131774
42	Normal	98	1000	No	EDTA		190927431
42	Tumor	108	941*	No	fixed	23	120828418
43	Normal	51	1000	Yes	EDTA		90620114
43	Tumor	158	373*	No	fixed	46	206945827
44	Normal	60	1000	Yes	EDTA		50917493
44	Tumor	42	1000	Yes	frozen	14	32736117
45	Normal	88	1000	No	EDTA		288287484
45	Tumor	108	292*	No	fixed	22	108587264

46	Normal	33	1000	Yes	EDTA		27281614
46	Tumor	40	1000	Yes	fixed	41	27533702
47	Normal	57	1000	Yes	EDTA		48624834
47	Tumor	16	1000	Yes	fixed	1	14145086

DNA input amount, whether library was overamplified, and estimated library size (unique molecules) per library.
 * estimated input amount.

Table S3 - COSMIC Cancer Gene Census genes

Gene	# samples
<i>TP53</i>	28
<i>PIK3CA</i>	14
<i>PIK3R1</i>	4
<i>CHD4</i>	3
<i>CACNA1D</i>	2
<i>NRAS</i>	2
<i>PTEN</i>	2
<i>AR</i>	1
<i>ARID1A</i>	1
<i>ATR</i>	1
<i>ATRX</i>	1
<i>BRAF</i>	1
<i>BRCA2</i>	1
<i>CASP8</i>	1
<i>DICER1</i>	1
<i>ERBB4</i>	1
<i>FGFR3</i>	1
<i>FLT3</i>	1
<i>IL6ST</i>	1
<i>JAK1</i>	1
<i>KDR</i>	1
<i>KEAP1</i>	1
<i>KMT2D</i>	1
<i>LRP1B</i>	1
<i>MAP3K13</i>	1
<i>MTOR</i>	1
<i>NCOR1</i>	1

<i>NFE2L2</i>	1
<i>NTRK3</i>	1
<i>PLCG1</i>	1
<i>RNF43</i>	1
<i>TERT</i>	1
<i>ZFHX3</i>	1

Genes mutated at least once in canine exome data, annotated as likely cancer drivers in the COSMIC Cancer Gene Census. Significantly mutated genes bolded.

Table S4 - RNA-seq validation

ID	Gene	Exome variant	Tissue preservation	Mutation type	VAF	Validated	RNA-seq pileup
17	ARPC1A	chr6:10238294:G:A	frozen	Nonsense	0.17	No	109 0:0:0:0:0:0:0:0
36	ARPC1A	chr6:10232318:A:C	fixed	Missense	0.16	Yes	283 0:0:36:0:0:1:0:0:0
21	ORC1	chr15:8982528:A:C	fixed	Missense	0.05	No	9 0:0:0:0:0:0:0:0
4	PIK3CA	chr34:12675674:A:T	frozen	Missense	0.25	No	67 0:0:0:11:0:0:0:0
18	PIK3CA	chr34:12651933:G:A	frozen	Missense	0.06	No	41 0:1:0:0:0:0:0:0
27	PIK3CA	chr34:12675674:A:G	fixed	Missense	0.23	No	38 0:0:0:1:0:1:0:0
28	PIK3CA	chr34:12675674:A:T	fixed	Missense	0.19	Yes	24 0:3:0:0:0:0:0:0
29	PIK3CA	chr34:12675674:A:G	fixed	Missense	0.11	Yes	29 0:0:0:11:0:0:0:0
11	PIK3CA	chr34:12675666:T:G	frozen	Missense	0.11	Yes	27 0:0:0:13:0:0:0:0
36	PIK3CA	chr34:12651893:G:A	fixed	Missense	0.15	Yes	35 10:0:0:0:0:0:0:0
21	PIK3R1	chr2:53522035:A:G	fixed	Missense	0.17	Yes	41 0:0:0:5:0:0:0:0
18	RASA1	chr3:21093342:G:A	frozen	Nonsense	0.11	No	43 0:1:0:0:0:0:0:0
28	RASA1	chr3:21108103:A:T	fixed	Nonsense	0.13	Yes	29 0:3:0:0:0:0:0:0
4	TP53	chr5:32563923:C:T	frozen	Missense	0.32	No	49 0:0:0:0:0:0:0:0
17	TP53	chr5:32563712:C:T	frozen	Missense	0.47	No	59 0:0:0:0:0:1:0:0
19	TP53	chr5:32563056:G:A	frozen	Missense	0.18	Yes	66 14:0:0:0:0:0:0:0
20	TP53	chr5:32563698:A:T	frozen	Missense	0.26	No	40 0:0:0:0:0:0:0:0
21	TP53	chr5:32563404:C:T	fixed	Missense	0.27	Yes	125 0:40:0:1:0:0:0:0
21	TP53	chr5:32564616:A:G	fixed	Missense	0.19	Yes	95 0:0:0:35:0:0:0:0
22	TP53	chr5:32563049:C:A	fixed	Missense	0.1	No	194 2:0:0:0:0:0:0:0
22	TP53	chr5:32563400:C:T	fixed	Missense	0.32	No	146 0:0:0:0:0:0:0:0
24	TP53	chr5:32563401:C:T	fixed	Missense	0.27	Yes	129 0:33:0:0:0:0:0:0
24	TP53	chr5:32563916:C:T	fixed	Missense	0.21	Yes	105 0:27:0:1:0:0:0:0
29	TP53	chr5:32563959:CCATAG:C	fixed	Frame shift	0.09	No	25 20:10:10:10:0:1:0:10:0
1	TP53	chr5:32561417:CG:C	fixed	Frame shift	0.17	No	82 0:0:0:15:0:2:0:14:0

1	TP53	chr5:32563056:G:A	fixed	Missense	0.07	Yes	52 14:0:0:0:2:0:0:0
11	TP53	chr5:32564027:G:A	frozen	Missense	0.42	Yes	147 116:0:0:0:2:0:0:0
13	TP53	chr5:32563400:C:T	frozen	Missense	0.42	Yes	198 0:148:0:0:0:0:0:0

Table S5 - RNA-seq survey

Gene	Golden	Boxer	GSD	Lab	PWD	Keeshond	Other	Total
TP53	18	0	1	0	2	1	1	23
PIK3CA	7	1	2	0	2	2	2	17
PIK3R1	2	0	0	1	1	0	1	5
ARPC1A	2	0	0	0	0	0	0	2

Survey of specific mutations identified in the exome sequencing in SMGs in RNA-seq data from canine angiosarcoma tumors in 43 golden retrievers and 31 dogs from other breeds.

Table S6 DAVID functional clustering analysis of human genes

See attached file.

Table S7 DAVID functional clustering analysis of canine genes

See attached file.

Table S8 DAVID functional clustering analysis of genes overlapping between human and canine

See attached file.

Table S9 DAVID functional clustering analysis of the union of genes between human and canine

See attached file.

Table S10 - somatic copy number aberrations by oaCGH

Gene	% with gain	% with loss
TP53	6	7
PIK3CA	10	4
PIK3R1	2	3
ORC1	7	2
RASA1	4	2
ARPC1A	2	0
ATP5H	0	0
PTEN	4	4

VEGFA	19	3
MYC	9	0
CDKN2A/B	0	22
KDR	22	0
KIT	17	0

Somatic copy number aberrations in SMGs, as well as in select genes reported to be recurrently altered in canine and human literature, in a cohort of 66 angiosarcomas analyzed by oaCGH. (Thomas, *et al.*, manuscript in preparation)(23).

Table S11 - comparison of top SCNAs in human Angiosarcoma Project data with canine oaCGH data

Gene	CNA	# patients	% altered (human)	% gain (golden retriever)	% loss (golden retriever)
OBSCN	DEL	15	42	6	15
KDR	AMP	13	36	22	0
DAXX	AMP	12	33	6	0
CD70	DEL	12	33	13	2
HOXA9	AMP	11	31	10	6
PPM1D	AMP	10	28	3	2
ZNF331	DEL	10	28	2	0
HOXA11	AMP	10	28	9	6
WWTR1	AMP	10	28	2	3
CD36	AMP	10	28	6	0
DDX5	AMP	10	28	9	0
TNFSF9	DEL	8	22	13	2
PTK2	AMP	8	22	6	2
MAP4K4	AMP	8	22	2	9
EGFL7	AMP	7	19	7	19
NDRG1	AMP	7	19	10	3
APH1A	AMP	7	19	4	0
KIT	AMP	7	19	17	0

Percentage copy number gain or loss in oaCGH data from 69 golden retriever angiosarcomas compared with the most frequent SCNAs (affecting >15% of patients) in 48 tumor samples from The Angiosarcoma Project. SCNAs affecting >15% of patients in the same direction in both species bolded. (Thomas, *et al.*, manuscript in preparation)(23).

Figure S1 - Canine exome sequencing workflow

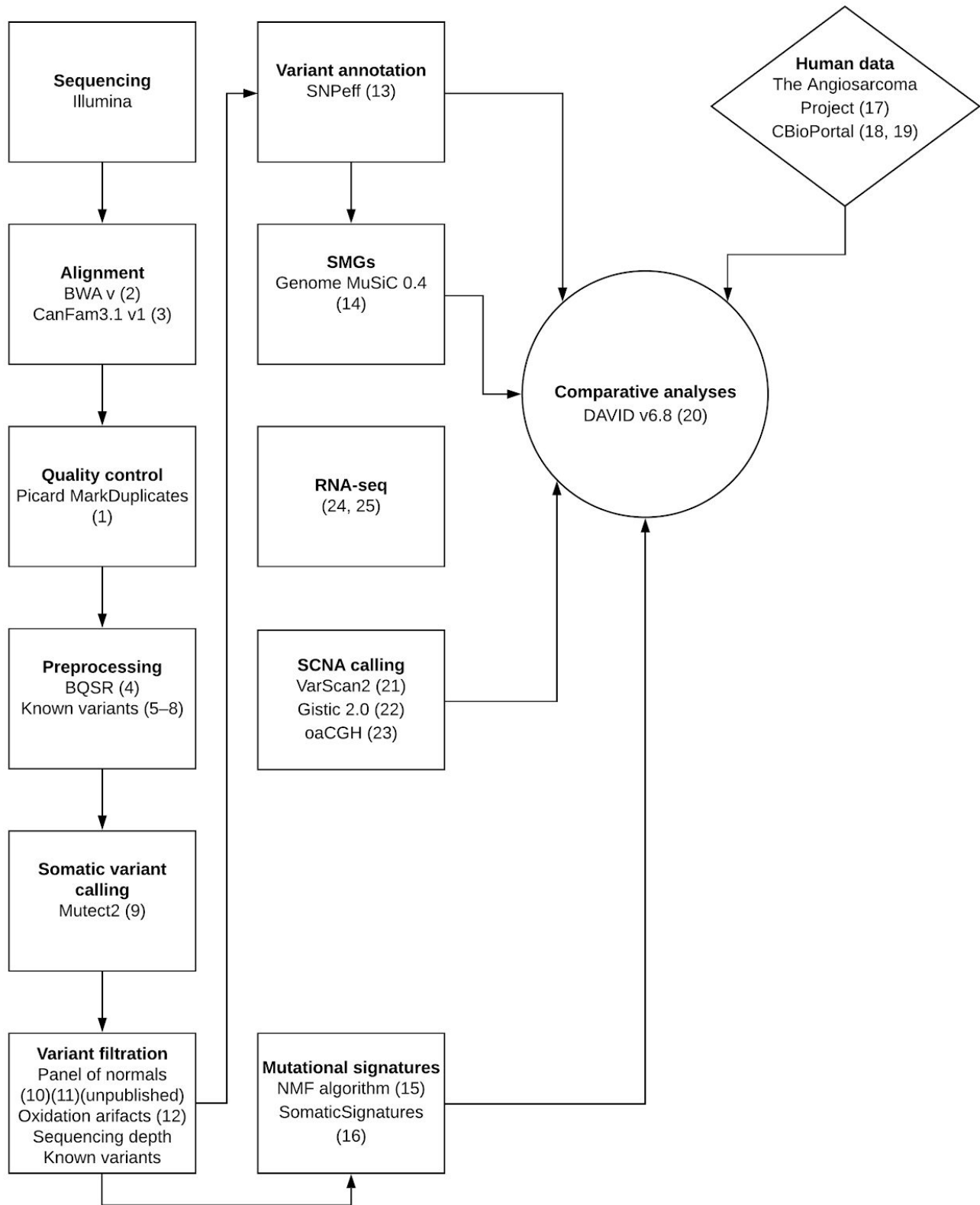


Figure S2 - SMGs called in overamplified vs. normal libraries

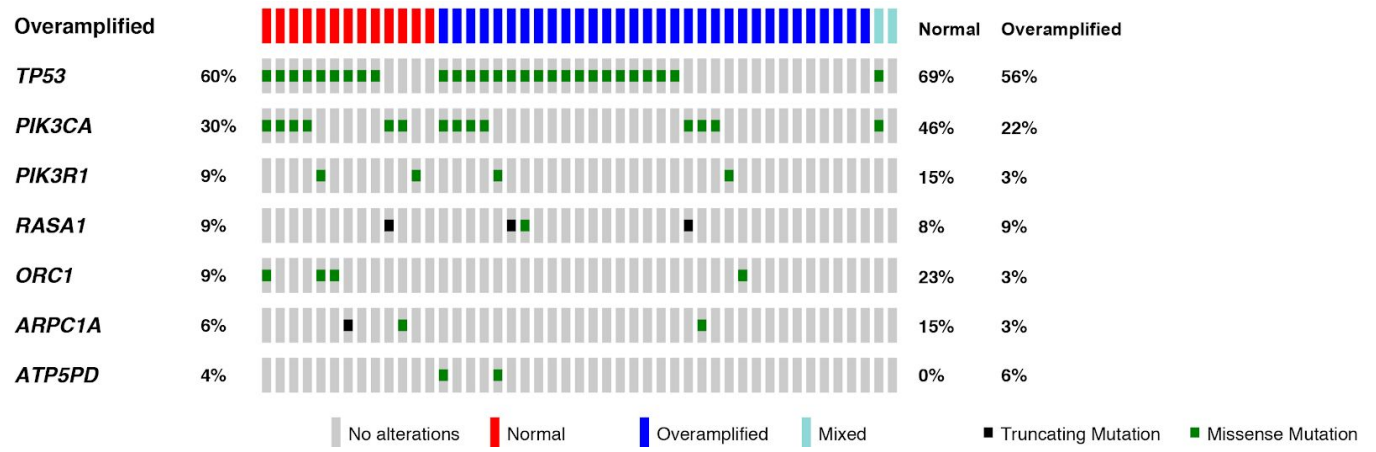
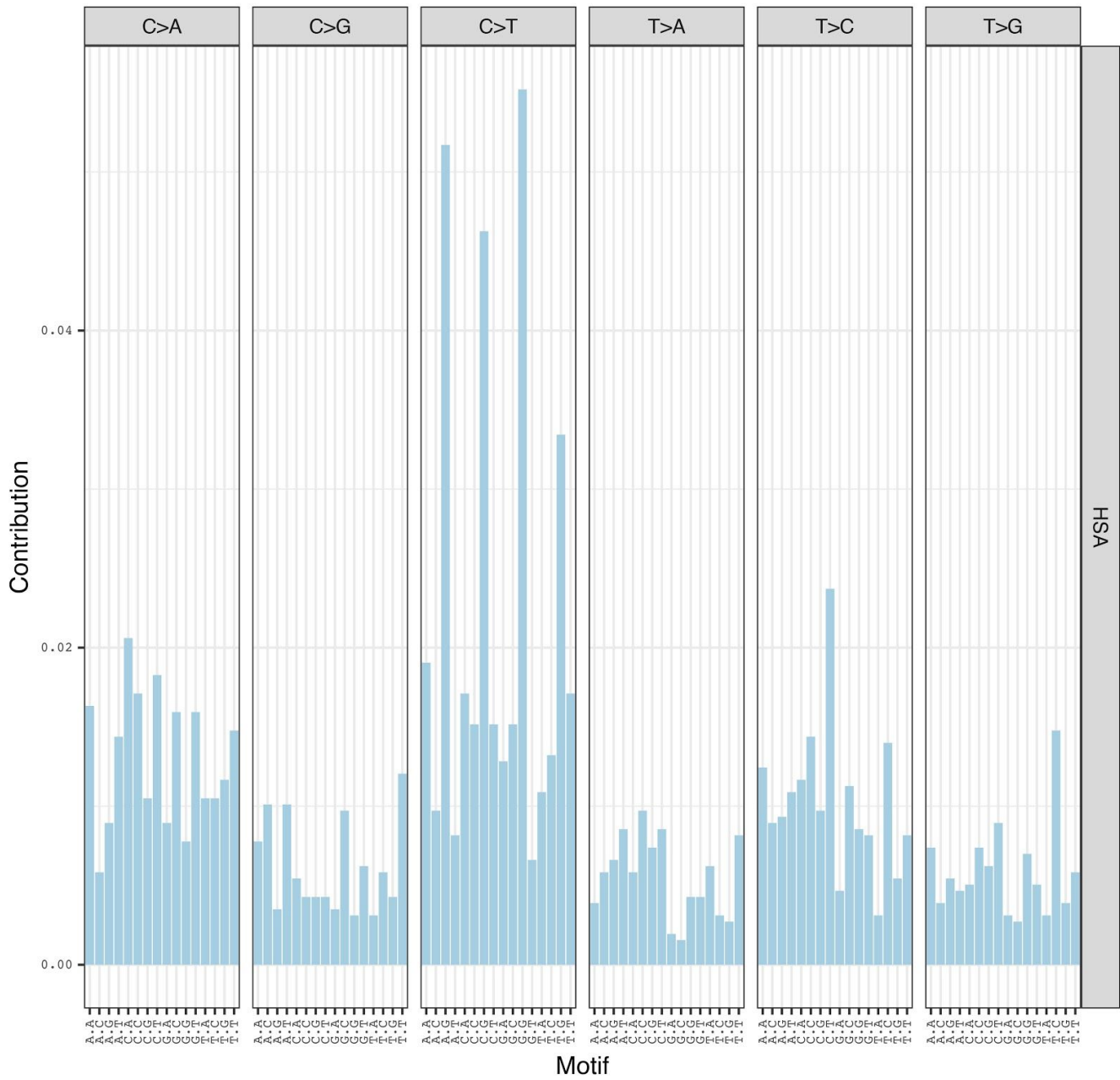
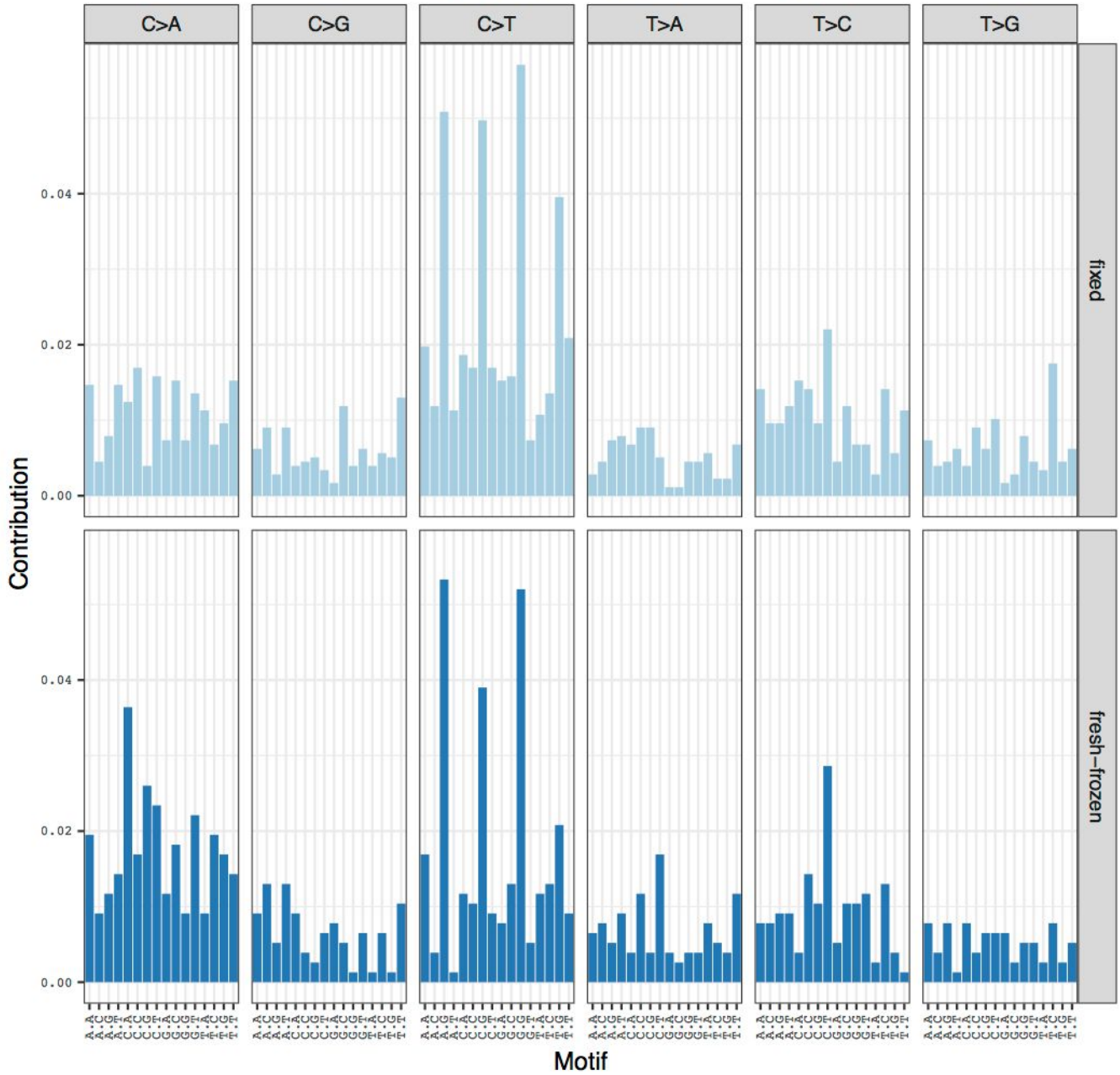


Figure S3 - Mutational landscape of entire cohort



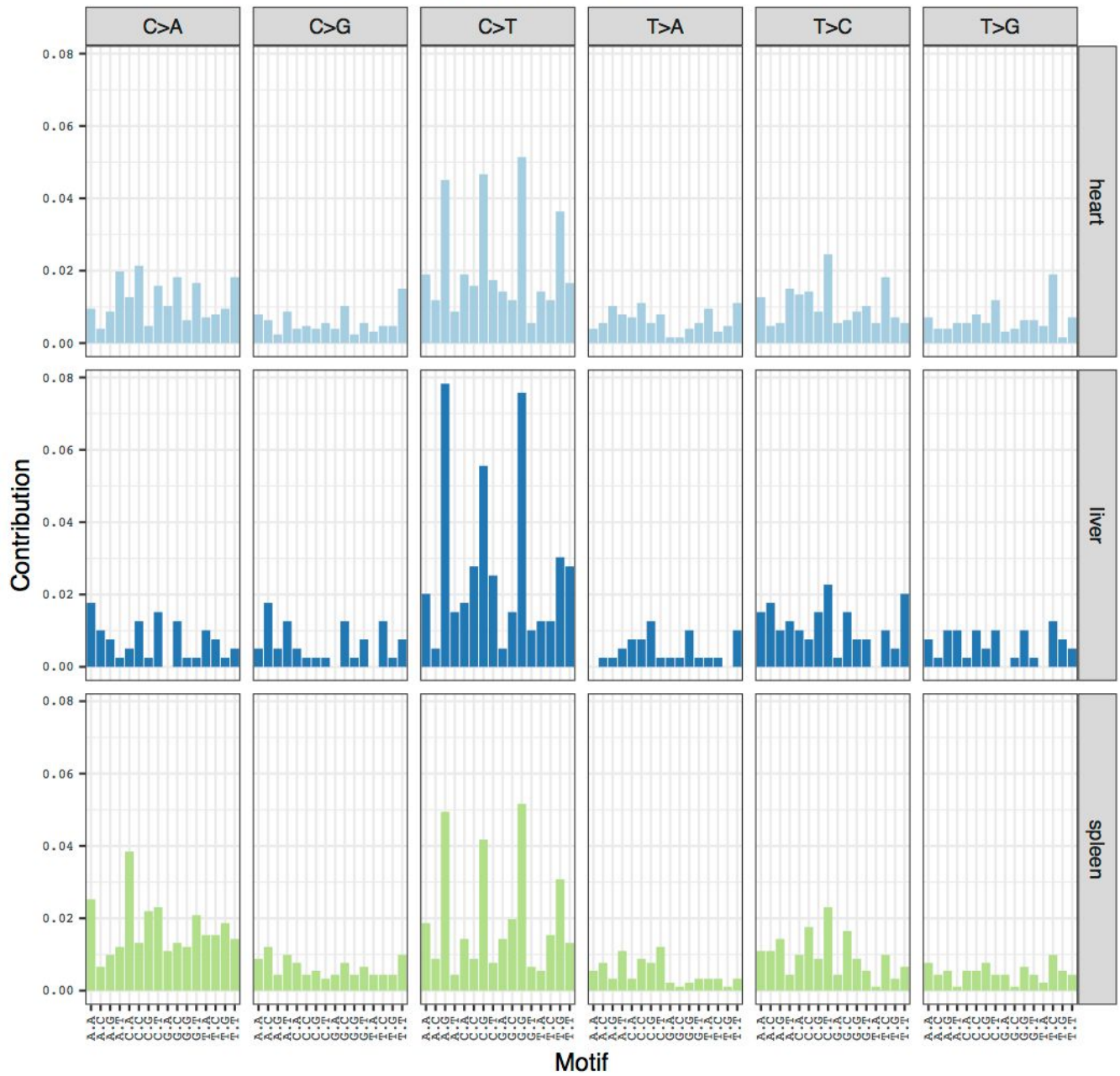
Mutational landscape of all canine angiosarcoma cases.

Figure S4 - Mutational landscape: FFPE vs Frozen



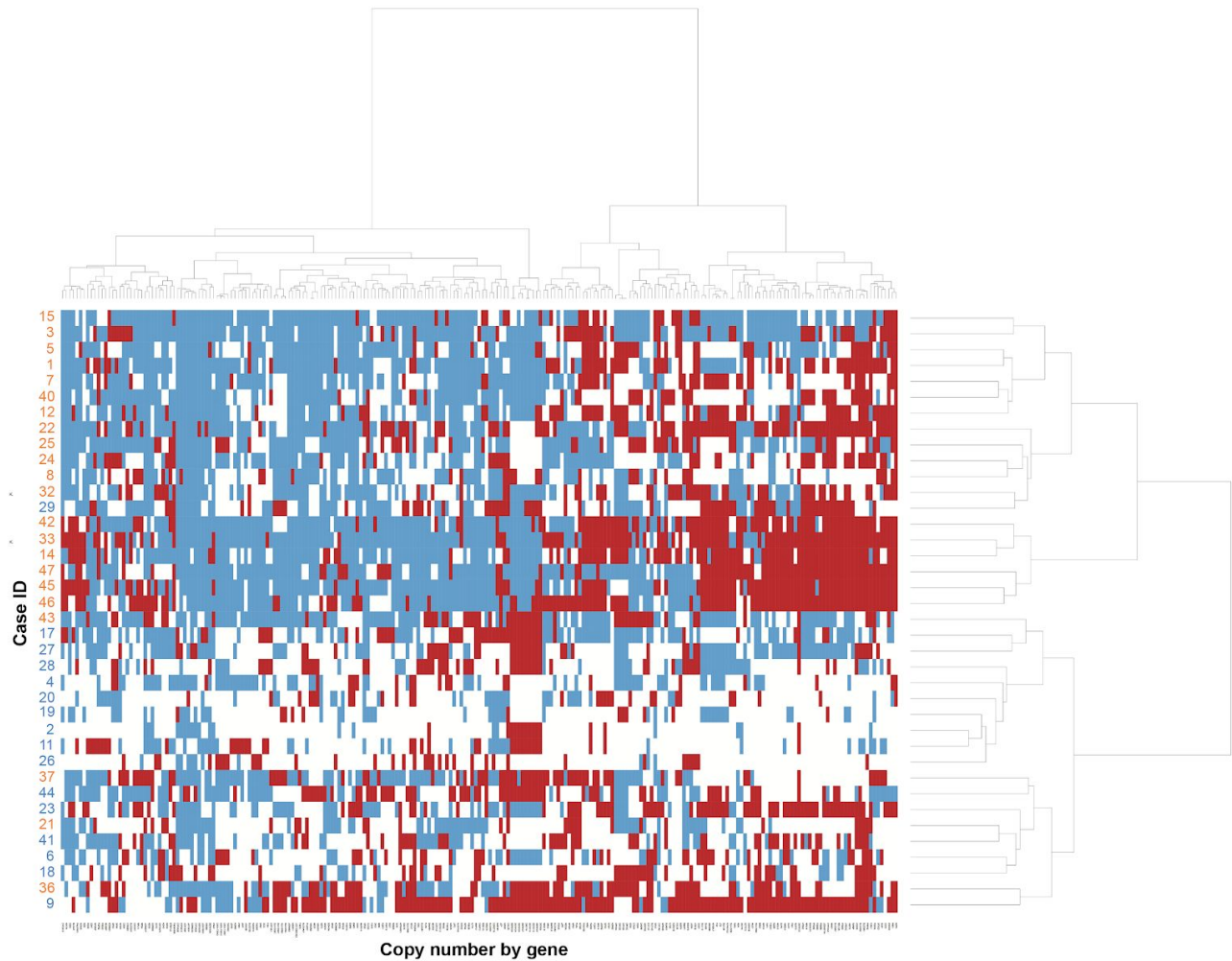
Mutational landscape of all canine cases, divided by tissue handling (fixed vs. frozen).

Figure S5 - Mutational landscape: Tumor Location



Mutational landscape of all canine cases, divided by tumor location (heart, liver, spleen).

Figure S6 - FFPE vs Frozen exome SCNA data clustering



Unsupervised clustering of the VarScan2 copy number aberrations in the 38 canine angiosarcoma cases with fewer than 10,000 segments, showing clustering of amplifications (red) and deletions (red) per gene by sample. Case IDs show fixed (orange) or frozen (blue) tissue.

References

1. Li H, Durbin R. Fast and accurate short read alignment with Burrows-Wheeler transform. *Bioinformatics*. 2009;25:1754–60.
2. Hoepfner MP, Lundquist A, Pirun M, Meadows JRS, Zamani N, Johnson J, et al. An improved canine genome and a comprehensive catalogue of coding genes and non-coding transcripts. *PLoS One*. 2014;9:e91172.
3. Picard Tools - By Broad Institute [Internet]. [cited 2018 Mar 23]. Available from: <http://broadinstitute.github.io/picard>
4. Van der Auwera GA, Carneiro MO, Hartl C, Poplin R, Del Angel G, Levy-Moonshine A, et al. From FastQ data to high confidence variant calls: the Genome Analysis Toolkit best practices pipeline. *Curr Protoc Bioinformatics*. 2013;43:11.10.1–33.
5. Lindblad-Toh K, Wade CM, Mikkelsen TS, Karlsson EK, Jaffe DB, Kamal M, et al. Genome sequence, comparative analysis and haplotype structure of the domestic dog. *Nature*. 2005;438:803–19.
6. Vaysse A, Ratnakumar A, Derrien T, Axelsson E, Rosengren Pielberg G, Sigurdsson S, et al. Identification of genomic regions associated with phenotypic variation between dog breeds using selection mapping. *PLoS Genet*. 2011;7:e1002316.
7. Axelsson E, Ratnakumar A, Arendt M-L, Maqbool K, Webster MT, Perloski M, et al. The genomic signature of dog domestication reveals adaptation to a starch-rich diet. *Nature*. 2013;495:360–4.
8. Bai B, Zhao W-M, Tang B-X, Wang Y-Q, Wang L, Zhang Z, et al. DoGSD: the dog and wolf genome SNP database. *Nucleic Acids Res*. 2015;43:D777–83.
9. Cibulskis K, Lawrence MS, Carter SL, Sivachenko A, Jaffe D, Sougnez C, et al. Sensitive detection of somatic point mutations in impure and heterogeneous cancer samples. *Nat Biotechnol*. 2013;31:213–9.
10. Elvers I, Turner-Maier J, Swofford R, Koltookian M, Johnson J, Stewart C, et al. Exome sequencing of lymphomas from three dog breeds reveals somatic mutation patterns reflecting genetic background. *Genome Res*. 2015;25:1634–45.
11. Sakthikumar S, Elvers I, Kim J, Arendt ML, Thomas R, Turner-Maier J, et al. SETD2 Is Recurrently Mutated in Whole-Exome Sequenced Canine Osteosarcoma. *Cancer Res*. 2018;78:3421–31.
12. Costello M, Pugh TJ, Fennell TJ, Stewart C, Lichtenstein L, Meldrim JC, et al. Discovery and characterization of artifactual mutations in deep coverage targeted capture sequencing data due to oxidative DNA damage during sample preparation. *Nucleic Acids Res*. 2013;41:e67.
13. Cingolani P, Platts A, Wang LL, Coon M, Nguyen T, Wang L, et al. A program for annotating and predicting the effects of single nucleotide polymorphisms, SnpEff: SNPs in the genome of *Drosophila melanogaster* strain w1118; iso-2; iso-3. *Fly*. 2012;6:80–92.
14. Dees ND, Zhang Q, Kandoth C, Wendl MC, Schierding W, Koboldt DC, et al. MuSiC: identifying mutational significance in cancer genomes. *Genome Res*. 2012;22:1589–98.
15. Kim J, Mouw KW, Polak P, Braunstein LZ, Kamburov A, Kwiatkowski DJ, et al. Somatic ERCC2 mutations are associated with a distinct genomic signature in urothelial tumors. *Nat Genet*. 2016;48:600–6.
16. Gehring JS, Fischer B, Lawrence M, Huber W. SomaticSignatures: inferring mutational signatures from

single-nucleotide variants. *Bioinformatics*. 2015;31:3673–5.

17. Corrie Painter NW. The Angiosarcoma Project [Internet]. [cited 2018 Sep 24]. Available from: <https://ascproject.org/>
18. Cerami E, Gao J, Dogrusoz U, Gross BE, Sumer SO, Aksoy BA, et al. The cBio cancer genomics portal: an open platform for exploring multidimensional cancer genomics data. *Cancer Discov*. 2012;2:401–4.
19. Gao J, Aksoy BA, Dogrusoz U, Dresdner G, Gross B, Sumer SO, et al. Integrative analysis of complex cancer genomics and clinical profiles using the cBioPortal. *Sci Signal*. 2013;6:11.
20. Dennis G Jr, Sherman BT, Hosack DA, Yang J, Gao W, Lane HC, et al. DAVID: Database for Annotation, Visualization, and Integrated Discovery. *Genome Biol*. 2003;4:P3.
21. Koboldt DC, Zhang Q, Larson DE, Shen D, McLellan MD, Lin L, et al. VarScan 2: somatic mutation and copy number alteration discovery in cancer by exome sequencing. *Genome Res*. 2012;22:568–76.
22. Mermel CH, Schumacher SE, Hill B, Meyerson ML, Beroukhi R, Getz G. GISTIC2.0 facilitates sensitive and confident localization of the targets of focal somatic copy-number alteration in human cancers. *Genome Biol*. 2011;12:R41.
23. Thomas R, Borst L, Rotroff D, Motsinger-Reif A, Lindblad-Toh K, Modiano JF, et al. Genomic profiling reveals extensive heterogeneity in somatic DNA copy number aberrations of canine hemangiosarcoma. *Chromosome Res*. 2014;22:305–19.
24. Gorden BH, Kim J-H, Sarver AL, Frantz AM, Breen M, Lindblad-Toh K, et al. Identification of three molecular and functional subtypes in canine hemangiosarcoma through gene expression profiling and progenitor cell characterization. *Am J Pathol*. 2014;184:985–95.
25. Tonomura N, Elvers I, Thomas R, Megquier K, Turner-Maier J, Howald C, et al. Genome-wide association study identifies shared risk loci common to two malignancies in golden retrievers. *PLoS Genet*. 2015;11:e1004922.